Chemical Methodologies 6(2022) 122-136

Chemical Methodologies

Journal homepage: http://chemmethod.com

Original Research Article

As Antimicrobial Agents: Synthesis, Structural Characterization and Molecular Docking Studies of Barbituric Acid Derivatives from Phenobarbital

Mahmood M. Fahad[1,*], Nusrat Shafiq[2], Uzma Arshad[2], Ali Jabbar Radhi[3]

[1]*Medical Laboratory Techniques Department, Kufa Technical Institute, Al-Furat Al-Awsat Technical University, Kufa, Iraq*
[2]*Department of Chemistry, Government College Women University Faisalabad-38000, Pakistan*
[3]*Faculty of Pharmacy, Al-Kafeel University, Najaf, Iraq*

ARTICLE INFO

Article history

Submitted: 2021-11-02
Revised: 2021-11-20
Accepted: 2021-11-22
Manuscript ID: CHEMM-2111-1391
Checked for Plagiarism: **Yes**
Language Editor:
Ermia Aghaie
Editor who approved publication:
Dr. Ghodsi Mohammadi Ziarani

DOI: 10.22034/chemm.2022.2.5

KEYWORDS

Barbituric acid
Phenobarbital
Cycloaddition reaction
Tetrazoline
Tetrazole

ABSTRACT

Despite phenobarbital having been used in various medical fields as hypnotics, anxiolytics, and anticonvulsants, it also contains active functional groups that can form dyes, polymers, antimicrobial, and anti-antioxidants agents. A series of barbituric acid derivatives containing 1,2,3,4-tetrazoline moiety were synthesized from phenobarbital. Phenobarbital 1 as raw starting material was reacted with acrylonitrile compound to give diacetonitrile derivative 2, this compound was treated in two ways, urea and thiourea to form barbituric acid derivatives containing oxadiazole and thiadiazole ring 3, 4 respectively. The Schiff bases derivatives 5, 6(a-c) were synthesized from reacting the latter compounds with three aromatic aldehydes. In the final step, the barbituric acid derivatives containing 1,2,3,4-tetrazoline moiety 7, $8_{(a\text{-}c)}$ were prepared by cycloaddition reaction between different Schiff bases derivatives and sodium azide. The synthesized compounds were characterized using melting point, ^{13}C-NMR, ^{1}H-NMR and FTIR techniques. The compounds were also tested against two kinds of bacteria and two kinds of fungi. Most of the prepared derivatives revealed a high and clear effect against different types of bacteria and fungi. Molecular docking of final barbituric acid derivatives 7, $8_{(a,\ b)}$ were investigated using Molegro Virtual Docker (MVD).

GRAPHICAL ABSTRACT

* Corresponding author: Mahmood M. Fahad
✉ E-mail: mahmood.mohy.iku@atu.edu.iq

Introduction

Due to their diverse biological effects, many barbituric acid derivatives have piqued the interest of the pharmaceutical community for more than a century [1]. Barbituric acids and their derivatives are organic substances that are utilized in pharmacology as hypnotics, sedatives, antihypertensive drugs, anesthetics, anticancer, anticonvulsants, antioxidants, antifungal agents, antibacterial, and Alpha-glycosidase enzyme inhibitors [2-7]. Chemically, via the donor-acceptor process of protons in the building-block structures of barbituric acid, the presence of five atoms (three oxygen and two nitrogen) with roles in coordination chemistry allows for the possible development and stability of supramolecular arrangements [8]. Barbituric acid can thus be defined as an organic building block that can behave intramolecularly and intermolecularly due to the presence of these O and N atoms [9]. Phenobarbital (PHB) or 5-ethyl, 5-phenyl barbituric acid as a starting material, is one of the most common barbituric acid derivatives. In their 1904 paper, Fischer and Dilthey listed phenobarbital compound as one of the compounds they discovered, Scheme 1 [10].

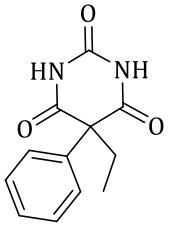

Scheme 1: Phenobarbital Compound

In organic chemistry, cycloaddition reactions are one of the most significant processes with synthetic and mechanistic importance. The simplicity of these cycloaddition reactions, as well as their exceptional stereochemistry, makes them useful [11]. 1,3-Dipolar cycloaddition reactions have been commonly used in the synthesis of natural products and bioactive organic compounds, as well as in the construction of various five-membered heterocyclic. The majority of 1,3-dipolar compounds are heteroatom based diazoalkanes, azomethine ylides, azides, nitrile ylides, nitrile imines, nitrile oxides, nitrones, carbonyl ylides, and carbonyl imines [12]. Tetrazole and its derivatives have a wide spectrum of biological activities, including antimicrobial, antifungal, HCV (Hepatitis C virus) inhibitor, potent hypoglycemic agent, and cholinesterase inhibitors [13-17]. Tetrazoline or substituted tetrazoline compounds have just one isomer and one carbon atom, but the tetrazoline has two tautomers, Scheme 2 [18].

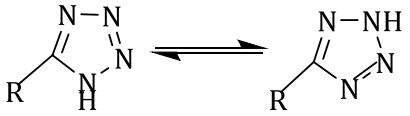

Scheme 2: Two tautomers of tetrazole

Experimental

The chemical materials and solvents were supplied and purchased from BDH (England), Fluke RDH (Switzerland), and Merck (Germany) Companies, Baghdad city. The Electro-thermal technique (SMP30) type was used to identify the melting points of the synthesized samples. The TLC test was measured to determine the progress of the reactions by using (glass TLC 1020 GS – Silica gel- 60). The synthesized compounds were characterized using (Shimadzu-8400S for IR; Kufa University, Bruker-75 MHZ, and 400 MHZ for NMR; Teheran, Iran). Biological activities were measured by using Petri dishes, Muller Hinton agar for bacteria test, potato agar for fungi test, and DMSO as solvent.

Chemical Part

Synthesis of 3,3'-(5-ethyl-2,4,6-trioxo-5-phenyldihydropyrimidine-1,3(2H,4H)-diyl) dipropanenitrile 2 [19]

In the presence of (0.012 mol) triethylamine, a mixture of (0.006 mol) phenobarbital 1 and

(0.012 mol) of acrylonitrile was mixed with (25 ML) of absolute ethanol. The contents were refluxed for 5 hrs. After that, the mixture was acidified by (0.1 N) of HCL to neutralize the mixture. The resulting product (85%) was filtered, washed and re-crystallized from acetone. Melting point: 170-172 °C, R_f: 0.55, TLC (4:1, Benzene: Methanol).

FT-IR spectra (ν_{max}): 2884-2972 cm^{-1} (Aliphatic CH), 2227 cm^{-1} (CN), 1660 cm^{-1} (C=O) Barbituric acid, ^{1}H-NMR Spectrum (DMSO-d_6): δ 3.81 (t, 4H, 2N-C$\underline{H}_2$), 3.18 (t, 4H, 2 C$\underline{H}_2$-CN), 2.28 (q, 2H, CH_2 Barbituric acid), 0.88 (t, 3H, CH_3 Barbituric acid), 7.28-7.48 (m, 5H, Aromatic ring-H), ^{13}C-NMR Spectrum (DMSO-d_6): 119.22 (2CN), 40.42 (2N-$\underline{C}H_2$), 16.14 (2$\underline{C}H_2$-CN), 150.23, 172.45 (3C=O) ppm, ^{13}C-NMR Spectrum (DMSO-d_6): δ 124.83, 128.48,140.23 ppm.

Synthesis of 1,3-bis(2-(5-amino-1,3,4-oxadiazol-2-yl) ethyl)-5-ethyl-5-phenylpyrimidine-2,4,6(1H,3H,5H)-trione 3 [20]

The compound 2 (0.006 mol) with (0.012 mol) of urea were mixed in (20 ML) absolute ethanol, the acetic acid was added drop by drop to the mixture. The reaction after refluxing 12 h was poured onto ice to give a white precipitate. The end result (78%) was washed with water and re-crystallized from Acetone. Melting point: 203-205 °C, R_f: 0.47, TLC (4:1, Benzene: Methanol).

FT-IR spectra (ν_{max}): 2738-2989 cm^{-1} (Aliphatic CH), 3331, 3381 cm^{-1} (NH_2 Sym, Asym), 1544 cm^{-1} (C-N), 1664 cm^{-1} (C=O) Barbituric acid. 1281 cm^{-1} (C-O), ^{1}H-NMR Spectrum (DMSO-d_6): δ 7.87 (s, 4H, 2NH_2), 3.34 (t, 4H, 2N-C$\underline{H}_2$), 2.67 (t, 4H, 2C$\underline{H}_2$-Oxidazole), 2.23 (q, 2H, CH_2 Barbituric acid), 0.86 (t, 3H, CH_3 Barbituric acid), 7.24-7.47 (m, 5H, Aromatic ring-H), ^{13}C-NMR Spectrum (DMSO-d_6): δ 156.59 (C-5 Oxadiazole), 163.61 (2C-NH_2), 43.65 (2N-$\underline{C}H_2$), 22.63 (2$\underline{C}H_2$-Oxidazole), 153.84, 175.42 (3C=O), 122.45, 125.01,143.60 ppm.

Synthesis of1,3-bis(2-(5-amino-1,3,4-thiadiazol-2-yl) ethyl)-5-ethyl-5-phenylpyrimidine-2,4,6(1H,3H,5H)-trione 4 [20]

As the previous compound 3, A (0.006 mol) of compound 2 and (0.012 mol) of thiourea were dissolved in (20 mL) of absolute ethanol. The acid (acetic acid) was added to the mixture. The reaction was refluxed for 12 hrs. The result precipitate (82%) was filtered, washed and re-crystallized from Acetone. Melting point: 198-200 °C, R_f: 0.5, TLC (4:1, Benzene: Methanol).

FT-IR spectra (ν_{max}): 2738-2989 cm^{-1} (Aliphatic CH), 3363 cm^{-1} (NH_2), 1541 cm^{-1} (C-N), 1669 cm^{-1} (C=O) Barbituric acid. 1274 cm^{-1} (C-O), ^{1}H-NMR Spectrum (DMSO-d_6): δ 7.85 (s, 4H, 2NH_2), 3.38 (t, 4H, 2N-C$\underline{H}_2$), 2.73 (t, 4H, 2C$\underline{H}_2$-Oxidazole), 2.19 (q, 2H, CH_2 Barbituric acid), 0.89 (t, 3H, CH_3 Barbituric acid), 7.20-7.52 (m, 5H, Aromatic ring-H), ^{13}C-NMR Spectrum (DMSO-d_6): δ 150.42 (C-5 Oxadiazole), 166.34 (2C-NH_2), 41.22 (2N-$\underline{C}H_2$), 20.37 (2$\underline{C}H_2$-Oxidazole), 155.72, 173.44 (3C=O), 119.32, 128.27,145.46 ppm.

General Synthesis of Schiff base derivatives 5, 6(a-c) [21-23]

A mixture of (0.006 mol) compounds (3 or 4) and (0.012 mol) of different aromatic aldehydes (4-(dimethylamino) benzaldehyde, 4-Bromobenzaldehyde and 2,4-Dichlorobenzaldehyde) were mixed with (20 ML) absolute ethanol. To the mixture, (3-4) drops of glacial acetic acid were added. For 6 hrs, the reaction was stirred and refluxed. The final products were washed with water, dried, and re-crystallized from hot ethanol, Table1.

FT-IR spectra (ν_{max}) for 5a: 1630 cm^{-1} (C=N imine), 1550 cm^{-1} (C=C aromatic). FT-IR spectra (ν_{max}) for 5b: 1643 cm^{-1} (C=N imine), 1547 cm^{-1} (C=C aromatic). FT-IR spectra (ν_{max}) for 5c: 1635 cm^{-1} (C=N imine), 1556 cm^{-1} (C=C aromatic).

^{1}H-NMR Spectrum for 5a (DMSO-d_6): δ 8.53 ppm (s, 1H, 2CH=N), 3.16 δ ppm (s, 3H, 2 N-C$\underline{H}_3$), 6.2-7.6 δ ppm (m, 4H, Aromatic ring-H), ^{1}H-NMR Spectrum for 5b (DMSO-d_6): δ 8.66 (s, 1H, 2CH=N), 6.5-7.9 (m, 4H, Aromatic ring-H), ^{1}H-NMR Spectrum for 5c (DMSO-d_6): δ 8.45 (s, 1H, 2CH=N), 6.8-7.7 (m, 4H, Aromatic ring-H), ^{13}C-NMR Spectrum (DMSO-d_6) for 5a: δ 160.55 (CH=N), 40.72 (N-$\underline{C}H_3$), ^{13}C-NMR Spectrum (DMSO-d_6) for 5b: δ 161.05 ppm (CH=N). ^{13}C-NMR Spectrum (DMSO-d_6) for 5c: 160.87 δ ppm (CH=N).

Table 1: General formula, M.wt, Reaction yield, M.p and R_f of compounds 5, $6_{(a-c)}$

Comp.	General formula	M.wt g\mol	Yield %	M.P ^{0}C	R_f
5a	$C_{38}H_{40}N_{10}O_5$	716.79	75%	140-142	0.53
5b	$C_{34}H_{28}Br_2N_8O_5$	788.44	83%	207-209	0.55
5c	$C_{34}H_{26}Cl_4N_8O_5$	768.43	80%	153-155	0.63
6a	$C_{38}H_{40}N_{10}O_3S_2$	748.92	77%	159-161	0.74
6b	$C_{34}H_{28}Br_2N_8O_3S_2$	820.58	78%	195-197	0.46
6c	$C_{34}H_{26}Cl_4N_8O_3S_2$	800.56	85%	166-169	0.49

General Synthesis of Barbituric acid Derivatives containing 1,2,3,4-Tetrazoline moiety ***7, 8(a-c)*** *[24-25]*

In the DMF solvent, the compounds 7, $8_{(a-c)}$ were prepared from reaction Schiff base derivatives 5, $6_{(a-c)}$, two moles of sodium azide, and catalytic agents (cupper chloride (I) with sodium ascorbate. At the room temperature, the reaction was stirred for 24 hrs. The reaction progress was followed by TLC technique (4:1, Benzene: Methanol). The results were filtered, dried, washed, and re-crystallized with ethanol, Table 2.

Table 2: General formula, M.Wt, Reaction yield, M.p and R_f of compounds 7, $8_{(a-c)}$

Comp.	General formula	M.Wt g\mol	Yield %	M.P ^{0}C	R_f
7a	$C_{38}H_{40}N_{16}Na_2O_5$	846.81	70%	174-176	0.65
7b	$C_{34}H_{28}Br_2N_{14}Na_2O_5$	918.46	74%	222-224	0.63
7c	$C_{34}H_{26}Cl_4N_{14}Na_2O_5$	898.45	80%	165-167	0.57
8a	$C_{38}H_{40}N_{16}Na_2O_3S_2$	878.94	76%	156-158	0.52
8b	$C_{34}H_{28}Br_2N_{14}Na_2O_3S_2$	950.60	71%	206-208	0.68
8c	$C_{34}H_{26}Cl_4N_{14}Na_2O_3S_2$	930.58	79%	177-178	0.66

FT-IR spectra (ν_{max}) for 7a: Disappearance (C=N imine) group, 1563 cm^{-1} (C=C aromatic), 1545 cm^{-1} (C=N) Oxadazole ring, 1147 cm^{-1} (C-N), 1058 cm^{-1} (N-N), 1679 cm^{-1} (C=O) Barbituric acid. FT-IR spectra (ν_{max}) for 7b: Disappearance (C=N imine), 1567 cm^{-1} (C=C aromatic), 1556 cm^{-1} (C=N) Oxadiazole ring, 1144 cm^{-1} (C-N), 1067 cm^{-1} (N-N), 1685 cm^{-1} (C=O) Barbituric acid. FT-IR spectra (ν_{max}) for 7c: Disappearance (C=N imine), 1574 cm^{-1} (C=C aromatic), 1539 cm^{-1} (C=N) Oxadiazole ring, 1172 cm^{-1} (C-N), 1076 cm^{-1} (N-N), 1668 cm^{-1} (C=O) Barbituric acid. ^{1}H-NMR Spectrum for 7a (DMSO-d_6): δ Disappearance (CH=N), 5.09 ppm (s, 2H, 2 CH), 3.40 ppm (s, 3H, 2 N-CH_3), 6.5-7.3 ppm (m, 4H, Aromatic ring-H), ^{1}H-NMR Spectrum for 7b (DMSO-d_6): Disappearance (s, 1H, 2CH=N), 5.06 ppm (s, 2H, 2 CH), 6.5-7.6 ppm (m, 4H, Aromatic ring-H), ^{1}H-NMR Spectrum for 7c (DMSO-d_6): Disappearance (s, 1H, 2CH=N), 5.12 δ ppm (s, 2H, 2 CH), 6.4-7.2 δ ppm (m, 4H, Aromatic ring-H), ^{13}C-NMR Spectrum (DMSO-d_6) for 7a: Disappearance (CH=N), 88.23 δ ppm (CH)mTetrazoline ring, 40.18 δ ppm (N-$\underline{C}H_3$), 112.34, 127.32, 136.35, 151.53 δ ppm (C-Aromatic ring). ^{13}C-NMR Spectrum (DMSO-d_6) for 7b: Disappearance (CH=N), 87.89 δ ppm (CH) Tetrazoline ring, 111.64, 128.92, 136.28, 153.26 δ ppm (C-Aromatic ring). ^{13}C-NMR Spectrum (DMSO-d_6) for 7c: Disappearance (CH=N), 85.03 δ ppm (CH) tetrazoline ring, 112.78, 128.05, 135.97, 151.89 δ ppm (C-Aromatic ring).

^{1}H-NMR Spectrum for 8a (DMSO-d_6): Disappearance (s, 1H, 2CH=N), 5.13 δ ppm (s, 2H, 2 CH), 3.34 δ ppm (s, 3H, 2 N-CH_3), 6.9-7.6 δ ppm (m, 4H, Aromatic ring-H), ^{1}H-NMR Spectrum for 8b (DMSO-d_6): Disappearance (s, 1H, 2CH=N), 5.23 δ ppm (s, 2H, 2 CH), 6.8-7.3 δ ppm (m, 4H, Aromatic ring-H), ^{1}H-NMR Spectrum for 8c (DMSO-d_6): Disappearance (s, 1H, 2CH=N), 5.16 δ ppm (s, 2H, 2 CH), 6.9-7.3 δ ppm (m, 4H, Aromatic ring-H),

^{13}C-NMR Spectrum (DMSO-d_6) for 8a: Disappearance (CH=N), 89.41 δ ppm (CH) Tetrazoline ring, 40.45 δ ppm (N-$\underline{C}H_3$), 112.35, 128.51, 136.63, 150.42 δ ppm (C-Aromatic ring). ^{13}C-NMR Spectrum (DMSO-d_6) for 8b: Disappearance (CH=N), 88.94 δ ppm (CH) Tetrazoline ring, 112.34, 127.54, 135.86, 152.99 δ ppm (C-Aromatic ring). ^{13}C-NMR Spectrum

(DMSO-d_6) for 8c: Disappearance (CH=N), 86.34 δ ppm (CH) Tetrazoline ring, 112.39, 128.52, 136.02, 152.29 δ ppm (C-Aromatic ring).

Biological part

The solutions were diluted by dissolving the chemically prepared compounds with dimethyl sulfoxide solvent to (0.05 gm.\ML). After the sterilization process of petri dishes at 140 ^{0}C for 1 h, every Petri dish was punctured into three equal holes (6 mm diameter) by a Cork borer. The dilute prepared compounds were placed in the holes for 24 h at 37 ^{0}C. Finally, the inhibition zones were measured by the ruler and compared the results with stander compounds [26-28]. The medium Muller Hinton Agar and potato dextrose agar were added to the petri dish as an active medium for the growth of the bacterial and fungal types respectively. The prepared compounds were tested against two kinds of bacteria ((*Staphylococcus aureus* (+) *& Escherichia coli* (-)) and two kinds of fungi (*Aspergillus flavus* & *Candida Albicans*).

Molecular Docking Methodology

Virtual molecular docking studies were used to investigate the inhibitory potential of produced compounds [29]. Virtual screening was performed using Molegro Virtual Docker (MVD), which was installed on an Intel Core i7 9700k processor with 120 GB SSD, 1 TB hard drive, and an NVIDA GeForce GTX 1050 graphics card [30, 31].

Preparation of Ligand

Following characterization, all synthesized structures were drawn using ChemDraw Professional 19.1 (PerkinElmer Inc, USA), and bond length and energy minimization were run on Chem3D Ultra 19.1.0.8 with the MMFF94 force field and imported to the MVD interface in mol2 format [32,33].

Homology Modelling

The protein sequence of Aspergillus flavus DNA-dependent RNA polymerase (RNAP) was retrieved from the NCBI database [34]. It was sent to the automated modeling website MODWEB, which was a comparative protein modeling web service for generating protein sequence modeling of RNAP by comparing the sequence to a template protein from *Schizosaccharomyces pombe* (PDB ID 3h0g) [35]. After computations, the theoretically modelled structure was evaluated and uploaded to MVD for docking [36], Table 3.

Preparation of target protein crystal

Protein 3D crystal structure was retrieved from the URL (http://www.rscb.org/pdb) [37-38]. Criteria for the selection of protein was based on the resolution greater than 1.5 A and containing the gene code of same bacterial and fungal specie, whose inhibition was required [39]. Protein co-crystal structure of same bacterial and fungal species were retrieved from PDB site which was also lined up for *in vitro* activities [36]. Table 3, depict the summary of proteins utilized in molecular docking [40]. Discovery studio visualizer was used for removing solvent/water molecules, along with heteroatom removal. As MVD executed the docking into active sites of protein structure, therefore extra chains were removed from protein [33, 36, 39]. Binding site sphere was generated, and protein was imported to MVD graphical interface. Surface was created and by using detects cavity preparation tools cavities were generated [41].

Molecular Docking and Scoring Function Assessment

Molegro Virtual Docker has user friendly graphical interface and relies on differential algorithm, which measures the protein-ligand interaction in the form of functional factor Rerank score for best docked pose [42,43]. While total energy of interaction between protein-ligand is measured in the form of MolDock score [44], based on PLP (pairwise linear potential) [33]. Grid resolution for docking was fixed to 0.30A, and binding site center co-ordinates was selected from user defined cavity 1 parameters [37]. Maximum iteration to 2000 and 50 maximum population size [29, 30]. Discovery Studio Visualizer was used for generation of 3D and 2D protein-ligand interactions [31, 45].

Table 3: Summary of protein used for molecular docking by MVD

Organism	PDB ID	Molecule
Staphlococcus aureus	1ad4	Dihydropteroate synthase
	3ttz	Topoisomerase ATPase inhibitor
Escherichia coli	6f86	*E. coli* DNA Gyrase in complex with pyridine-3-carboxamide
	1kzn	DNA gyrase in complex with coumarin based inhibitor
Aspergillus fumigatus	6drs	Dihydrofolate reductase (DHFR) complex with small inhibitor
	Homology modelled	DNA dependent RNA polymerase
Candida albican	1ai9	*C. albicans* dihydrofolate reductase
	4hof	Dihydrofolate reductase

Results and Discussion

Chemistry

The main goal of the study is to prepare and characterize new barbituric acid derivatives that contain tetrazoline moiety, which is an active moiety in pharmaceutical compounds. The first step involved preparing a 3,3'-(5-ethyl-2,4,6-trioxo-5-phenyldihydropyrimidine-1,3(2H,4H)-diyl) dipropanenitrile from the sreaction of phenobarbital with acrylonitrile in the presence of triethylamine as base catalyst, Scheme 3.

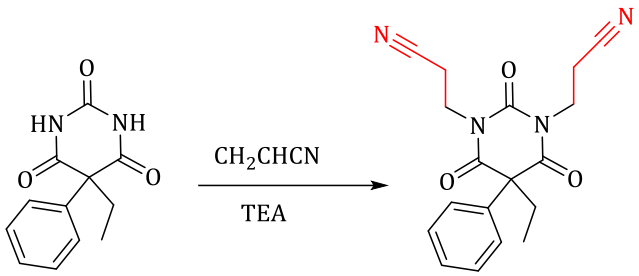

Scheme 3: Synthesis of diacetonitrile derivative

According to the anti-Markovnikov rule, the N-H group is added to the carbon-carbon of an alkene during the hydroamination reaction of an inactivated alkene. FT-IR Spectrum, the (CN) as a distinct group was observed at 2227 cm^{-1}. While in the ^{1}H-NMR, the peaks were observed at 3.50 ppm for (N-CH_2) and 3.15 ppm for (CH_2-CN).^{13}C-NMR Spectrum was was given 119.22 ppm for (CN), 40.42 ppm for (N-CH_2) and 16.14 ppm for (CH_2-CN). Barbituric acid derivatives containing 1,3,4-oxadiazole and 1,3,4-thiadiazole ring 3, 4 were formed by reacting diacetonitrile derivative 2 with urea and thiourea. The mechanism of the reaction is similar in both steps; the difference is in the oxygen and sulfur atoms. The (NH_2) group in FTIR was notified at 3381 cm^{-1} and 3363 cm^{-1}. In ^{1}H-NMR, these compounds were given the peaks: 7.87-7.85 ppm for (NH_2), 3.34-3.38 ppm for (N-CH_2), 2.67-2.73 ppm for (CH_2-Oxidazole). These are clear guides to form the compounds 3, 4, Scheme 4.

With drops of glacial acetic acid as a catalyst, the compounds 3 and 4 interact with various aldehydes such as (4-(dimethylamino) benzaldehyde, 4-Bromobenzaldehyde, and 2,4-Dichlorobenzaldehyde). In the Schiff base reactions 5, 6, the distinguishing group in Schiff-Base reactions is (C=N). The FT-IR peaks at 1630 cm^{-1}, 1643 cm^{-1}, and 1635 cm^{-1} corresponded to the (C=N imine) group respectively. The (CH=N) was detected as a single in the ^{1}H-NMR spectrum at 8.53 ppm, 8.66 ppm, and 8.45 ppm. The (CH=N) was found at 160.55 ppm, 161.05 ppm, and 160.87 ppm, respectively. While, in the ^{13}C-NMR spectrum, the (CH=N) group was noticed at 160.55, 161.05, 160.87 δ ppm respectively, Scheme 5.

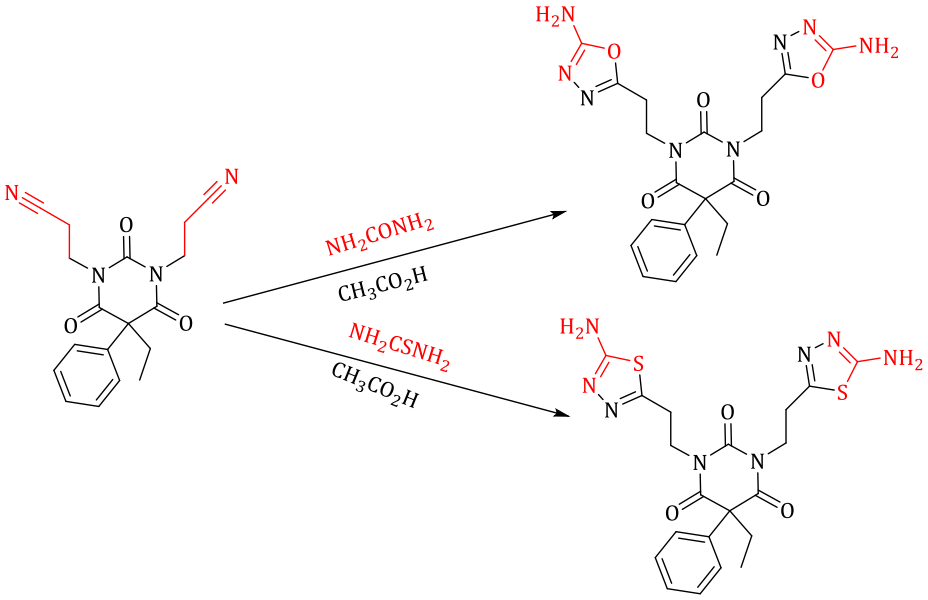

Scheme 4: Synthesis of Barbituric acid containing Oxadiazole and Thiadiazole ring

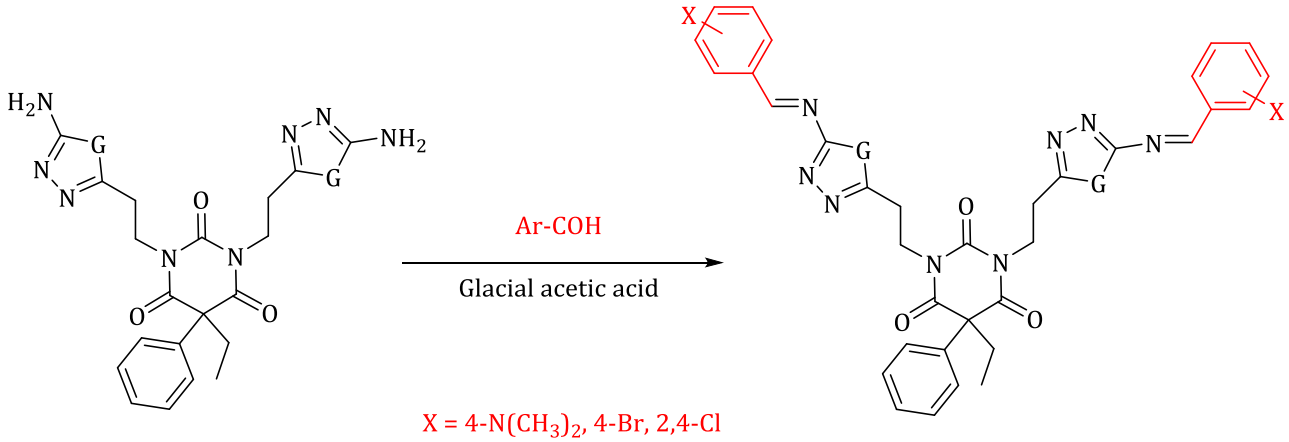

Scheme 5: Synthesis of Schiff bases derivatives

In the final step, the dipolarophile products from the Schiff bases were reacted with the 1,3- dipole (sodium azide) by [3+2] cycloaddition reaction in the presence of catalysts as copper chloride Cu (I) and sodium ascorbate to form barbituric acid derivatives containing 1,2,3,4-Tetrazoline moiety 7, 8(a-c). It is noticed that the imine (C=N) and azide (-N_3) groups disappear from Schiff bases and sodium azide spectra with new peaks are formed, Scheme 6.

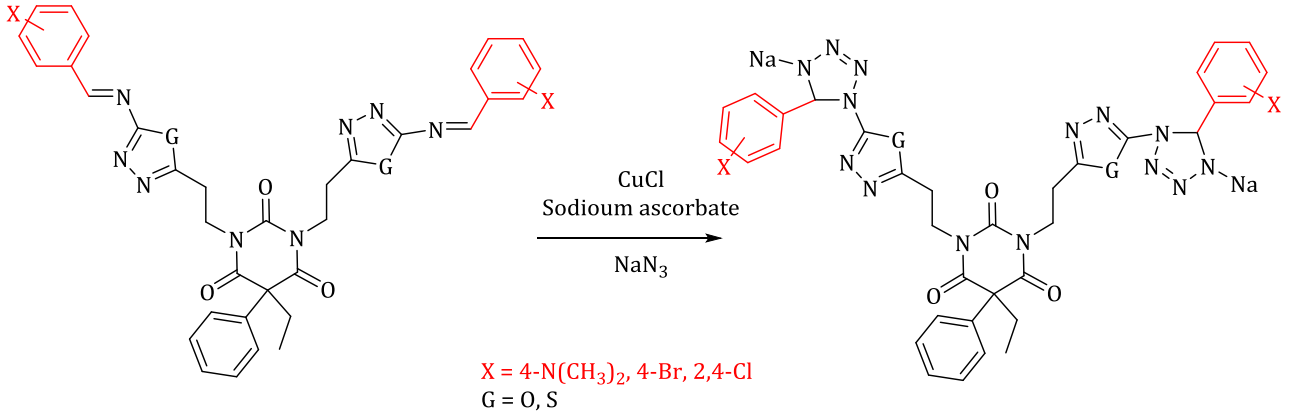

Scheme 6: Synthesis of barbituric acid derivatives

Biological Activity in vitro

The main goal of the work is the results of the applications of the prepared compounds; the tetrazoline derivatives have many applications in the field of medicine. From this point, these new derivatives were prepared to give high efficacy against bacteria and fungi types. The chemical prepared derivatives 7, 8 (a, b) were examined against two kinds of bacteria ((*Staphylococcus aureus* (+) *& Escherichia coli* (-)) and two kinds of fungi (*Aspergillus flavus* & *Candida Albicans*) by using Muller Hinton Agar and Potato Dextrose Agar. The biological results of prepared compounds with standard compounds are recorded in the following Table 4 and Figure 1.

Table 4: Antimicrobial test of some prepared compounds **7, 8** **(a, b)**

Sample	Antibacterial		Antifungal	
	S. aureus	***E. coli***	***A. flavus***	***C. Albicans***
Phenobarbital	+	+	-	-
7a	++	++	+++	+++
7b	-	-	+++	+++
8a	++	++	+++	+++
8b	++	++	+++	+++
Ampicillin	+++	+++	+	-
Fluconazole	+	+	+++	+++

Where, - = Resistant, + = 1-10 cm, ++ = 10-20 cm, +++ = 20-30cm.

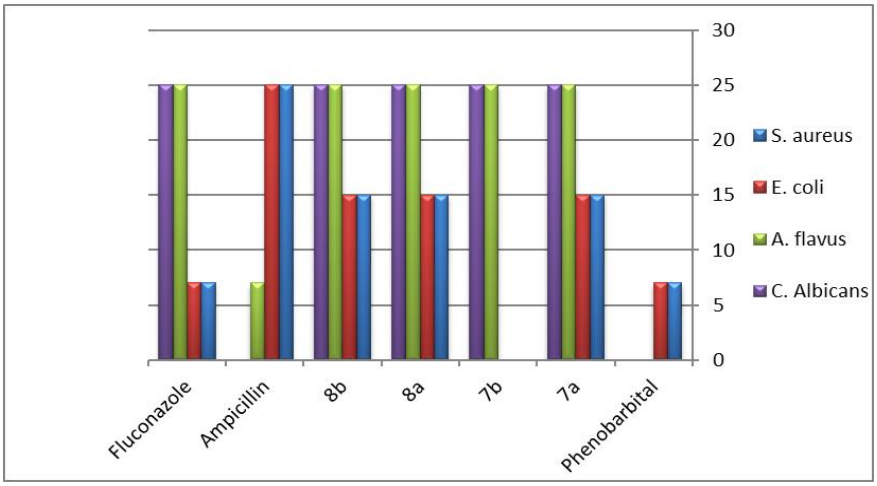

Figure 1: Antimicrobial test of some prepared compounds 7, 8(a, b)

It is noted in the Table 4 and Figure 1 that the raw material represented by phenobarbital compound gave a low active against bacteria types, while in the fungi types it was inactive. All compounds 7,8 (a, b) gave high activity against types of fungi and equal to the standard compound (Fluconazole). The compounds (7a, 8a-b) also gave moderately active against all bacteria types, while the compound (7b) was inactive at (0.05 gm/mL).

Molecular Modelling

In molecular docking antimicrobial targets was selected based on known mechanism of action of marketed antibiotic drugs.

All synthesized compounds (7a, 7b, 8a, and 8b) were docked to the binding cavity 1 of DNA gyrase, topoisomerase and dihydropteroate synthetase of *E. coli* and *S. aureus* respectively. While antifungal *in silico* studies was carried out into the active sites of RNA polymerase, dihydrofolate reductase of *A. flavus.* Active sites of antifolates and dihydrofolates from *C. albicans* were inhibited by docking the synthesized compounds. Tables 5 and 6 display the interaction energies in the form of MolDock score and the number of protein-ligand interactions in the form of Re-rank score. The Best established docked pose was selected based on MolDock score, the number of hydrogen bond interactions, hydrophobic and Van der Waals (VdW) interactions [37].

Compound 7a behaves a potential lead against *S. aureus*, as it showed maximum MolDock score for topoisomerase ATPase and DNA gyrase having three hydrogen bond interactions with DNA gyrase and ten hydrogen bond interactions with

topoisomerase ATPase. Also showed best MolDock score against dihydrofolate reductase of C. albican with twelve hydrogen bond interactions. All these interactions involved oxygen, nitrogen, methylene hydrogens and hydrogen of diethyamino moieties [46].

Compound 7b showed a high MolDock score against RNA polymerase and dihydrofolate reductase of *A. flavus*. Thus, possessing the best inhibiting potential for *A. flavus*. As these results were in accordance with *in vitro* antimicrobial activity. It had four hydrogen bond interactions to the active sites of RNA polymerase from oxygen and nitrogen atoms. With dihydrofolate reductase 7b has six hydrogen bond interactions. 7b also showed alkyl and pi-alkyl interactions with the bromo atom [38].

Compound 8a acts the lead compound with highest MolDock score for inhibiting the growth of antifolates of *A. flavus* and dihydropteroate synthetase of *S. aureus* respectively. 8a showed six hydrogen bond interactions along with six different types of interactions comprising VdW, hydrogen bond, pi-donor, pi-lone pair, and alkyl interactions with dihydropteroate synthesize. Antifolate showed total of four hydrogen bond interactions [31].

Compound 8b inhibited the growth of DNA gyrase of *E. coli,* having six hydrogen bond interactions involving oxygen and nitrogen atoms. While other interactions involved halogen, pi-donor and pi-alkyl [41].

Table 5: Molecular Docking against bacterial Strains

	Molecular Docking against bacterial Strains							
	S. aureus				*E. coli*			
Proteins	Dihydropteroate synthetase From S. aureus		Topoisomerase ATPase		DNA Gyrase complex with pyridine-3-carboxamide		DNA Gyrase complex with Clorobiocin	
Comp.	MolDock Score (kcal/mol)	Re-rank score	MolDock Score (kcal/mol)	Re-rank score	MolDock Score (kcal/mol)	Re-rank score	MolDock Score (kcal/mol)	Re-rank score
7a	-174.76	5.087	-191.83	-105.82	-175.30	13.30	-191.83	-105.82
7b	-159.75	-71.22	-173.16	-110.77	-185.48	-106.39	-154.50	-35.13
8a	-179.61	-82.33	-171.35	-119.09	-179.00	-95.30	-155.15	-51.92
8b	-164.82	-77.68	-175.23	-102.16	-190.191	-96.44	-160.58	7.05
Ampicillin	-100.33	-45.22	-201.43	-82.62	-110.27	-69.02	-88.04	-56.85

Table 6: Molecular Docking against Fungal Strains

	Molecular Docking against Fungal Strains							
	A. flavus				*C. albican*			
Proteins	Dihydrofolate Reductase with small inhibitor		RNA polymerase		dihydrofolate reductase		Dihydrofolate Reductase	
Comp.	MolDock Score (kcal/mol)	Re-rank score (kcal/mol)	MolDock Score (kcal/mol)	Re-rank score (kcal/mol)	MolDock Score (kcal/mol)	Re-rank score (kcal/mol)	MolDock Score (kcal/mol)	Re-rank score (kcal/mol)
7a	-235.13	-175.90	-192.76	-131.19	-144.09	-49.28	-228.72	-95.72
7b	-237.13	-150.38	-194.60	-126.30	-160.29	-76.52	-170.68	-96.80
8a	-230.31	-169.44	-188.51	-106.55	-161.40	-92.40	-172.16	-23.26
8b	-155.96	-77.22	-178.52	-95.54	-174.93	-81.82	-153.78	-40.75
Fluconazole	-109.58	-90.09	-107.68	-75.12	-106.44	-81.51	-85.20	-61.84

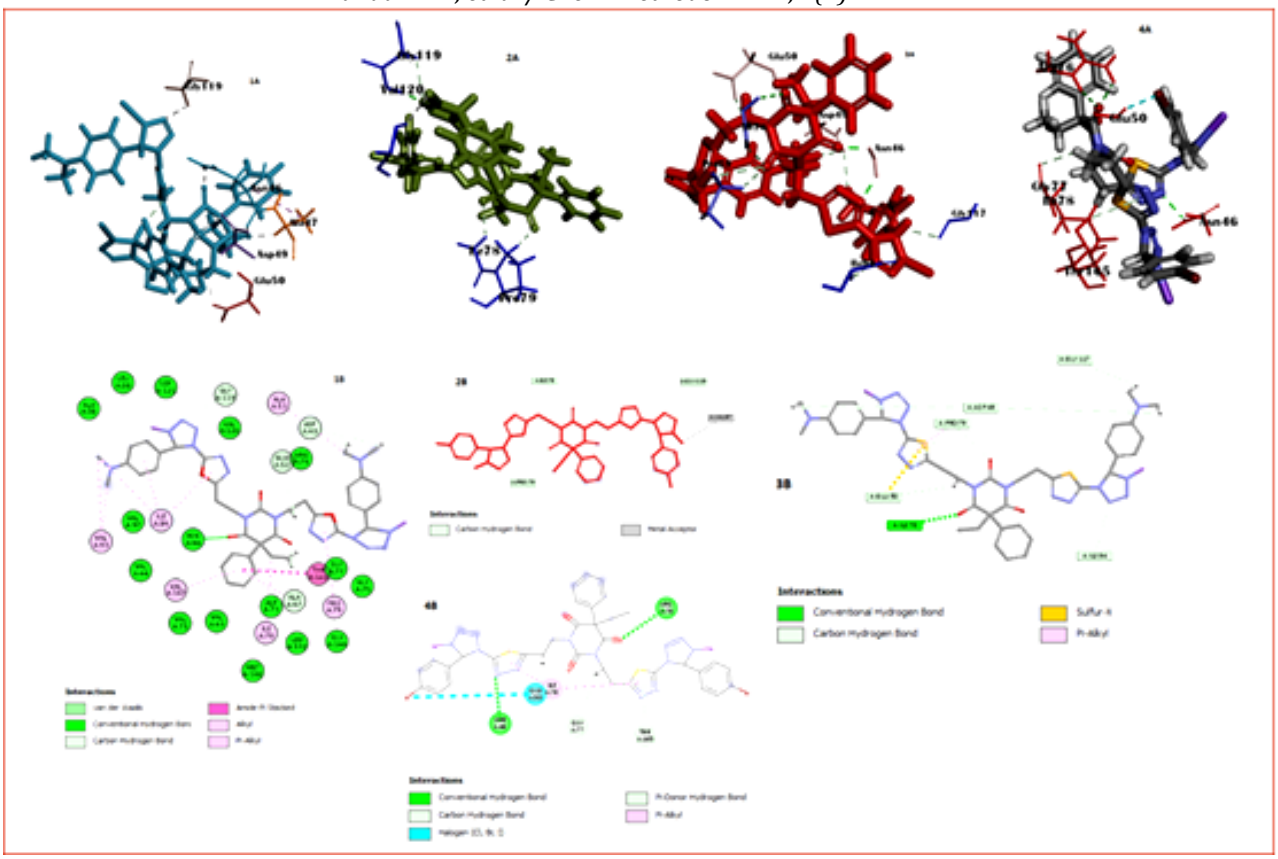

Figure 2: Three-dimensional view of compounds 7a-8b from 1A-4A (1A=7a, 2A=7b, 3A=8a, 4A=8b) into the binding cavity of 6f86, 2D view by Discovery studio of compounds 7a-8b from 1B-4B (1B=7a, 2B=7b, 3B=8a, 4AB=8b) for 6f86 (DNA Gyrase of E. coli)

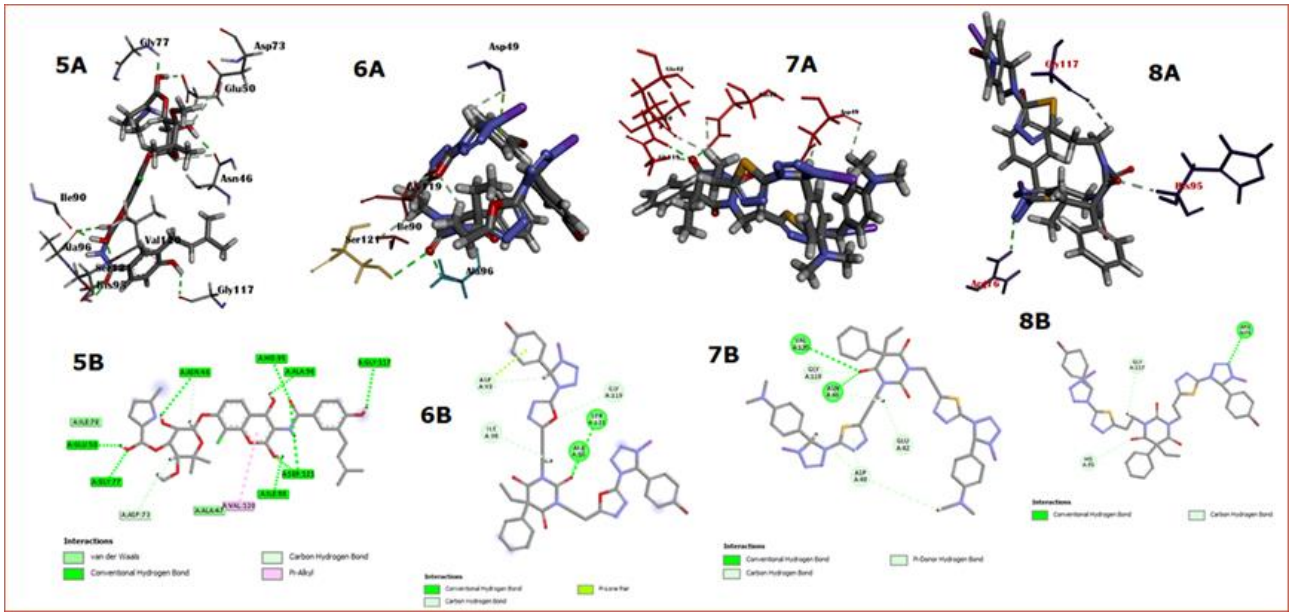

Figure 2: Three-dimensional view of compounds 7a-8b from 5A-8A into the binding cavity of 1kzn, 2D view by Discovery studio of compounds 7a-8b from 5B-8B for 1kzn (DNA Gyrase of S. aureus)

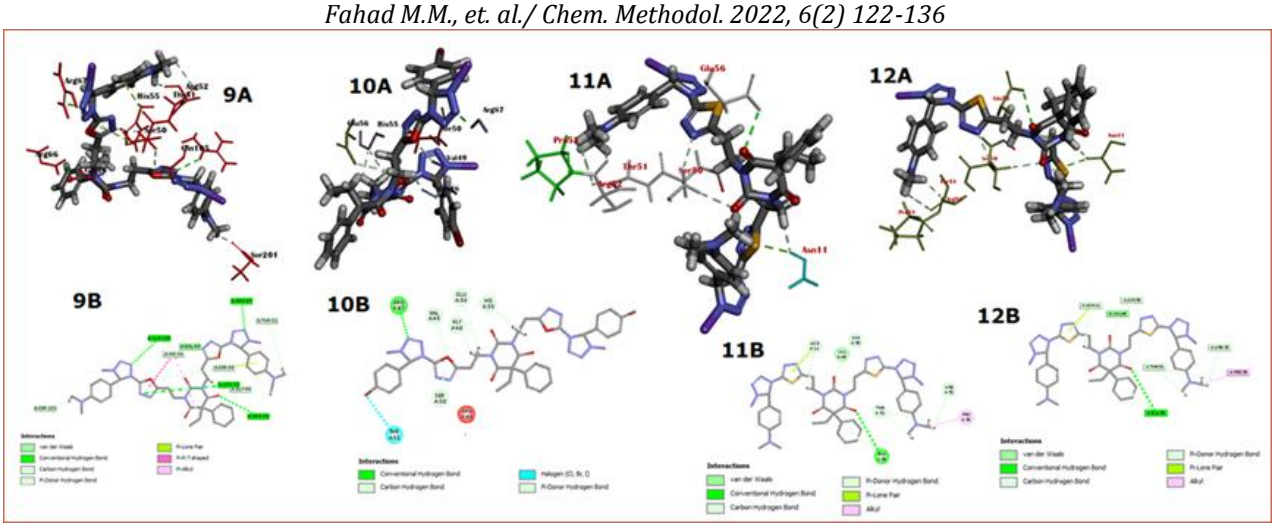

Figure 3: Three-dimensional view of compounds 7a-8b from 9A-12A into the binding cavity of 1ad4, 2D view by Discovery studio of compounds 7a-8b from 9B-12B for 1ad4 (dihydropteroate synthetized of S. aureus)

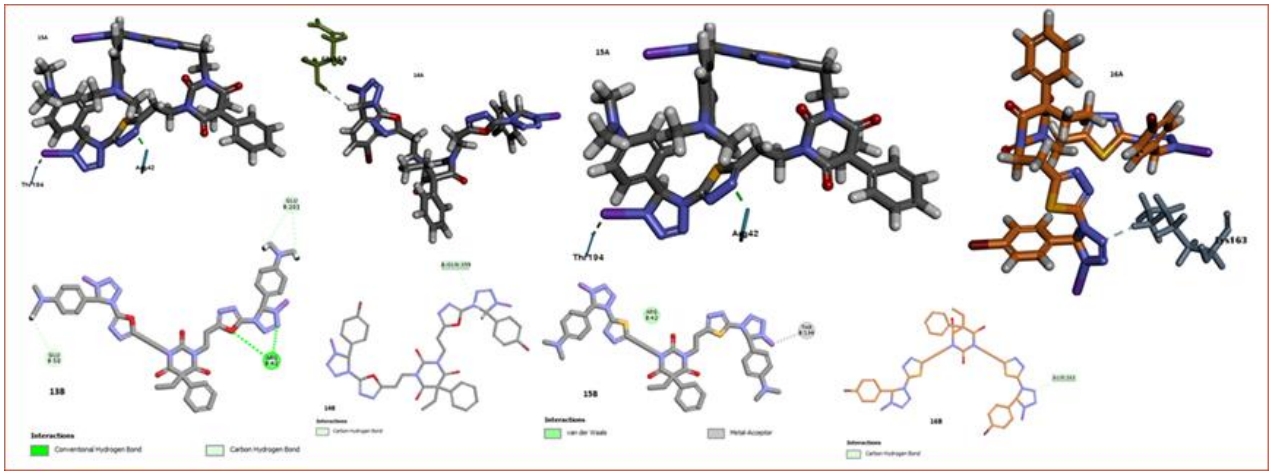

Figure 4: Three-dimensional view of compounds 7a-8b from 13A-16A into the binding cavity of 3ttz, 2D view by Discovery studio of compounds 7a-8b from 13B-16B for 1ad4 (topoisomerase ATPase of S. aureus)

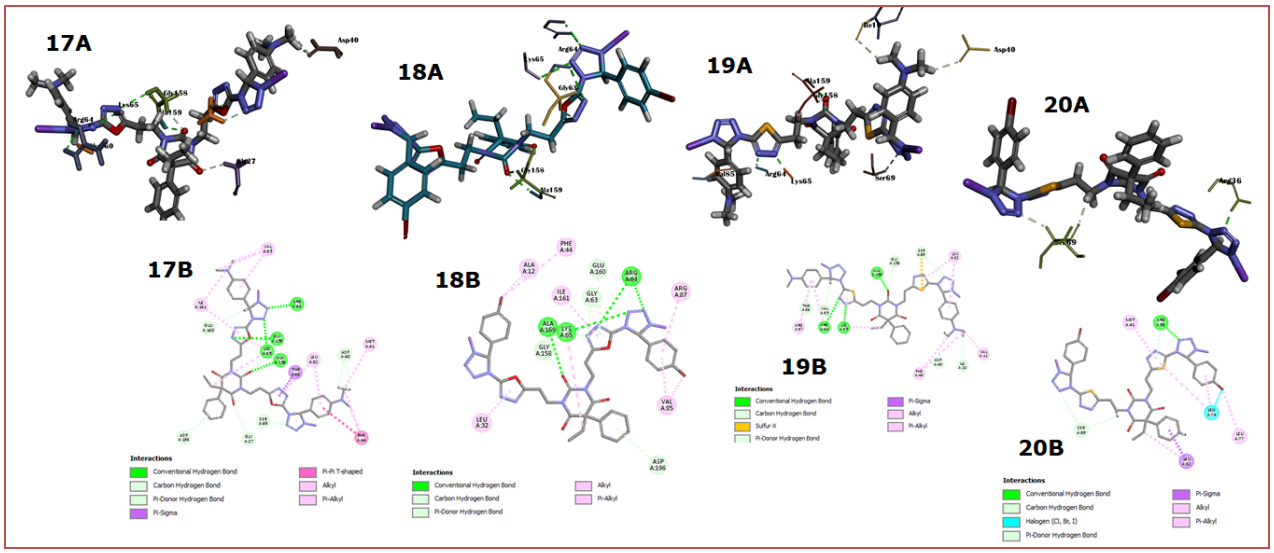

Figure 5: Three-dimensional view of compounds 7a-8b from 17A-20A into the binding cavity of 6drs, 2D view by Discovery studio of compounds 7a-8b from 17B-20B for 6drs (dihydrofolate reductase of A. flavus)

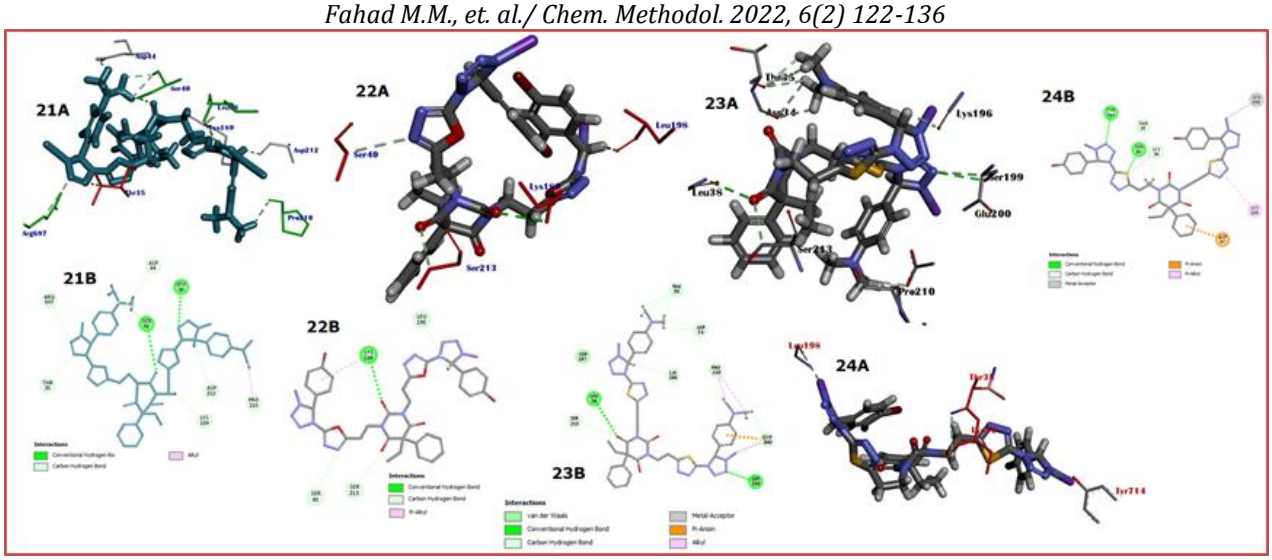

Figure 6: Three-dimensional view of compounds 7a-8b from 21A-24A into the binding cavity of 6drs, 2D view by Discovery studio of compounds 7a-8b from 21B-24B for homology modelled protein (RNA polymerase of A. flavus)

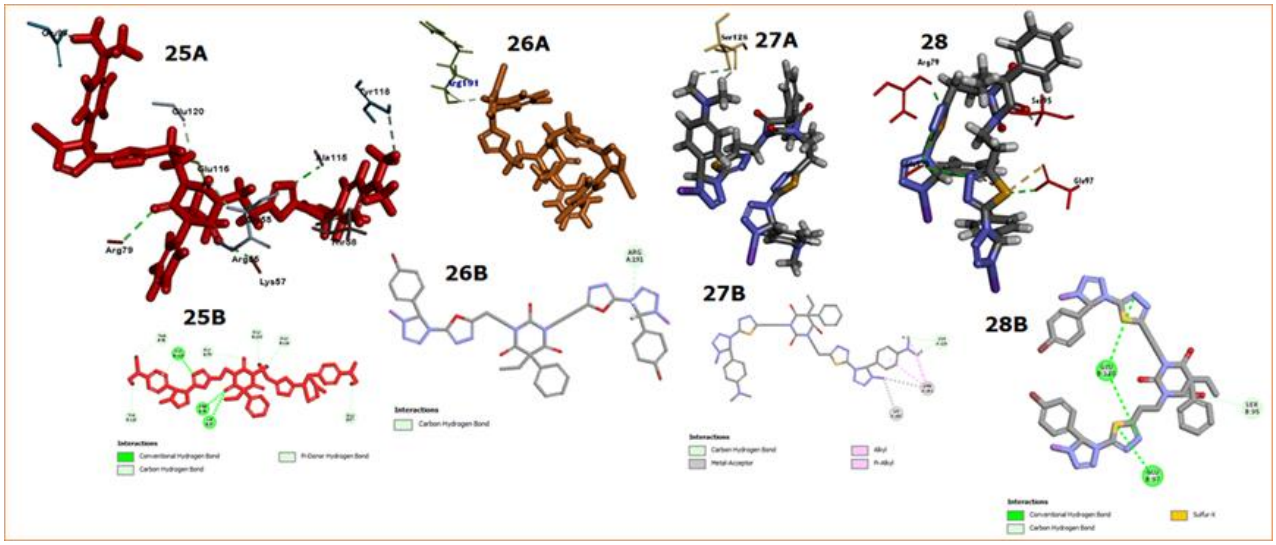

Figure 7: Three-dimensional view of compounds 7a-8b from 25A-28A into the binding cavity of 6drs, 2D view by Discovery studio of compounds 7a-8b from 25B-28B for 1ai9 (dihydrofolate reductase of C. albicans)

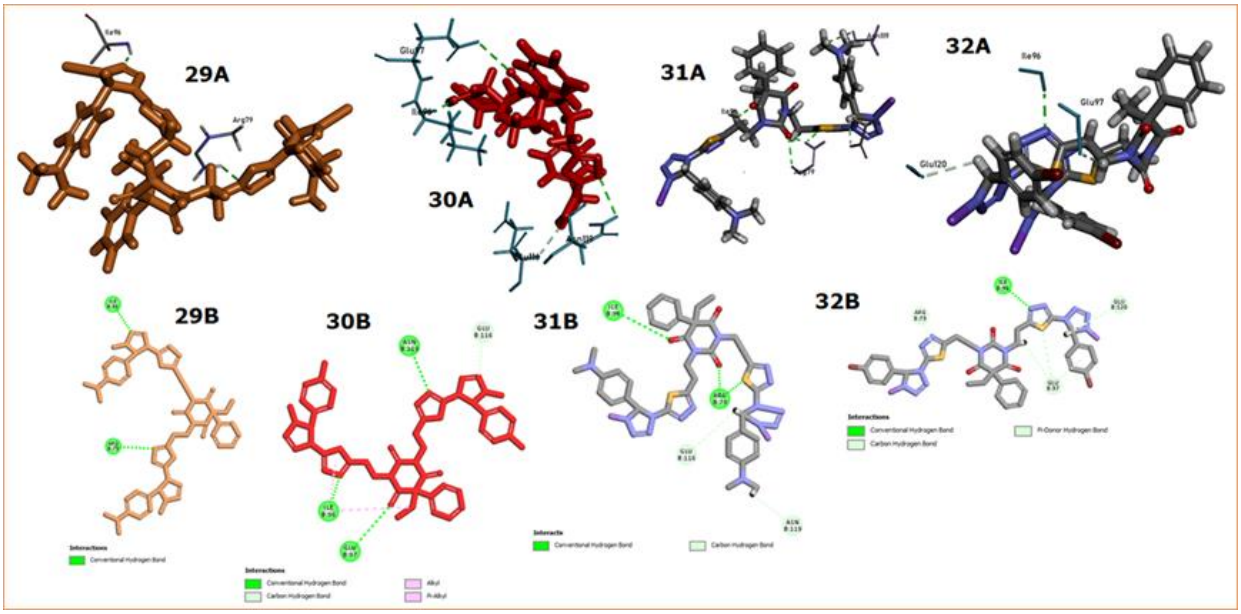

Figure 8: Three-dimensional view of compounds 7a-8b from 29A-32A into the binding cavity of 6drs, 2D view by Discovery studio of compounds 7a-8b from 29B-32B for 4hof (dihyrofolate reductase of C. albicans)

Conclusion

Barbituric acid and tetrazole or tetrazoline compounds are important in various medical applications. Phenobarbital as raw material was used to make a series of barbituric acid derivatives containing 1,2,3,4-tetrazoline moiety. The resulting compounds were characterized by various techniques as (melting point, TLC, FT-IR, ^{1}H-NMR, and ^{13}C-NMR). In the antifungal test, all results were given high activity against types of fungi and equal to the standard compound (Fluconazole), however in the antibacterial test; they showed a wide range of activities and low values when compared to the standard compound (Ampicillin). All these results corroborate the in vitro antimicrobial activity also, as the compounds which were inactive in antimicrobial activity also showed less MolDock score in the silicon study also. These compounds showed the best hydrophobic interactions along with hydrogen bonds thus hypothesizing that these interactions were important for the stabilization of the protein-ligand complex [47]. After antimicrobial docking simulation, we concluded that compound 7a can be an antimicrobial lead compound as an inhibitor of DNA and nucleic acid synthesis [48].

Acknowledgments

All thanks and appreciation to the pharmacist Tuqa S. Al-Amin for completing the biological applications.

Funding

This research did not receive any specific grant from funding agencies in the public, commercial, or not-for-profit sectors.

Authors' contributions

All authors contributed toward data analysis, drafting and revising the paper and agreed to be responsible for all the aspects of this work.

Conflict of Interest

We have no conflicts of interest to disclose.

ORCID

Mahmood M. Fahad:
https://orcid.org/0000-0003-2405-7047
Nusrat Shafiq:
https://orcid.org/0000-0002-3270-4227
Uzma Arshad:
https://orcid.org/0000-0003-4694-7761
Ali Jabbar Radhi:
https://orcid.org/0000-0002-7578-1716

References

[1]. David W., Thomas L., Lippincott, *Foye's Principles of Medicinal Chemistry* (5th ed) Williams & Wilkins, 2002 [Publisher]
[2]. Abbas H.K., Obaid E.K., Salman F.W., Shaheed H.A., Radhi A.J., *International Conference on Materials Engineering & Science*, 2020, **2213**:1 [Crossref], [Google Scholar], [Publisher]
[3]. Kolev T., Bakalska R., Seidel R.W., Mayer-Figge H., Oppel I.M., Spiteller M., Sheldrick W.S., Koleva B.B., *Tetrahedron: Asymmetry*, 2009, **20**:327 [Crossref], [Google Scholar], [Publisher]
[4]. Ali J.R., Ezzat H.Z., Emad A.J.A., *Research J. Pharm. and Tech*., 2019, **12**:1145 [Crossref], [Publisher]
[5]. Venkateswaran A., Reddy Y.T., Sonar V.N., Muthusamy V., Crooks P.A., Freeman M.L., Sekhar K.R., *Bioorganic Med. Chem. Lett.*, 2010, **20**:7323 [Crossref], [Google Scholar], [Publisher]
[6]. Mahmudov K.T., Kopylovich M.N., Maharramov A.M., Kurbanova M.M., Gurbanov A.V., Pombeiro A.J., *Coord. Chem. Rev.*, 2014, **265**:1 [Crossref], [Google Scholar], [Publisher]
[7]. Krasnov K.A., Dorovatovskii P.V., Zubavichus Y.V., Timofeeva T.V., Khrustalev V.N., *Tetrahedron*, 2017, **73**:542 [Crossref], [Google Scholar], [Publisher]
[8]. Garcia H.C., Campos M.T., Edwards H.G., de Oliveira L.F., *Vib. Spectrosc.*, 2016, **86**:134 [Crossref], [Google Scholar], [Publisher]
[9]. Thetford D., Chorlton A.P., Hardman J., *Dyes and Pigments*, 2003, **59**:185 [Crossref], [Google Scholar], [Publisher]
[10]. Louis D.Q., John A.T., Fundamentals of heterocyclic chemistry (10 ed) John Wiley, 2010, 112 [Google Scholar], [Publisher]
[11]. Aurell M.J., Domingo L.R., Pérez P., Contreras R., *Tetrahedron*, 2004, **60**:11503 [Crossref], [Google Scholar], [Publisher]
[12]. Li J.Q., Liao R.Z., Ding W.J., Cheng Y., *J. Org. Chem*., 2007, **72**:6266 [Crossref], [Google Scholar], [Publisher]

[13]. Khitam T.A.A., Suaad M.H.A., Oday H.R.A., *Iraqi J. Sci.*, 2016, **57**:295 [Google Scholar], [Publisher]
[14]. Mohite P.B., Bhaskar V.H., *J. Optoelectron. Biomed. Mater.*, 2011, **3**:87 [Google Scholar], [Publisher]
[15]. Rajasekaran A., Thampi P.P., Eur., *J. Med. Chem.*, 2005, **40**:1359 [Crossref], [Google Scholar], [Publisher]
[16] Adamec J., Waisser K., Kuneš J., Kaustová J., *Arch. Pharm. Chem. Life Sci*., 2005, **338**:385 [Crossref], [Google Scholar], [Publisher]
[17]. Shanmugam G., Bhakiaraj D., Elavarasan S., Elavarasan T., Gopalakrishan M., *Chem. Sci. Trans.*, 2013, **2**:1304 [Crossref], [Google Scholar], [Publisher]
[18]. Clayden J., Nick G., Stuart W., Peter W., *Organic chemistry*, 2007, 1168 [Publisher]
[19]. Sonwane S.K., Srivastava S.D., *J. Sci. Islam. Repub.*, 2009, **20**:227 [Publisher]
[20]. Mermer A., Bayrak H., Şirin Y., Emirik M., Demirbaş N., *J. Mol. Struct.*, 2019, **1189**:279 [Crossref], [Google Scholar], [Publisher]
[21]. Srivastava A.K., Yadav P., Srivastava K., Prasad J., *Chem. Data Collect.*, 2021, **32**:100659 [Crossref], [Google Scholar], [Publisher]
[22]. Mahato S., Meheta N., Kotakonda M., Joshi M., Shit M., Choudhury A.R., Biswas B., *Polyhedron,* 2021, **194**:11493 [Crossref], [Google Scholar], [Publisher]
[23]. Sharaby C.M., Amine M.F., Hamed A.A., *J. Mol. Struct.*, 2016, **1134**:208 [Crossref], [Google Scholar], [Publisher]
[24]. Rezaei F., Amrollahi M.A., Khalifeh R., *Inorganica Chim. Acta*, 2019, **489**:8 [Crossref], [Google Scholar], [Publisher]
[25]. Manzoor S., Cao W.L., Zhang J.G., *Def. Technol.*, 2021, **9**:1 [Crossref], [Google Scholar], [Publisher]
[26]. Zeyrek C.T., Arpacı Ö.T., Arısoy M., Onurdağ F.K., *J. Mol. Struct.*, 2021, **5**:1 [Crossref], [Google Scholar], [Publisher]
[27]. Ego rove N.S., *Antibiotics Scientific Approach.* Mir publishers, Moscow, 1985 [Publisher]
[28]. Mahmood M.F., Ezzat H.Z., Majed J.M., *Nano Biomed. Eng*., 2019, **1**:124 [Google Scholar], [Publisher]
[29]. Jin Z., Du X., Xu Y., Deng Y., Liu M., Zhao Y., Zhang B., Li X., Zhang L., Peng C.J.N., *Nature*, 2020, **582**:289 [Crossref], [Google Scholar], [Publisher]
[30]. Kim Y., Jedrzejczak R., Maltseva N.I., Wilamowski M., Endres M., Godzik A., Michalska K., Joachimiak A.J., *Protein Sci*., 2020, **29**:1596 [Crossref], [Google Scholar], [Publisher]
[31]. Reddy N.N., Hung S.J., Swamy M.K., Sanjeev A., Rao V.S., Rohini R., Raju A.K., Bhaskar K., Hu A., Reddy P.M., *Molecules*, 2021, **26**:1952 [Crossref], [Google Scholar], [Publisher]
[32]. Ayik R.P., *Int. Curr. Pharm. J.,* 2014, **3**:265 [Crossref]
[33]. Bernardi D.M., Marchi J.P., Araújo C.D., do Nascimento V.R., de Souza Lima D., Wietzikoski S., Ferro M.M., Miyoshi E., dos Reis Lívero F.A., Seixas F.A., Lovato E.C., *Res. Soc. Dev.*, 2021, **10** [Crossref], [Google Scholar], [Publisher]
[34]. Thambidurai P., Raja V., Ashokapuram S. S., Kannaiyan M., Shanmugam, *Appl. Sci.*, 2019, **9**:2485 [Crossref], [Google Scholar], [Publisher]
[35]. Webb B., Sali A., *Curr. Protoc. Bioinformatics*, 2016, **54**:1 [Crossref], [Google Scholar], [Publisher]
[36]. Zakaria N.H., WAI L., Hassan N.I., *Sains Malaysiana*, 2020, **49**:1905 [Crossref], [Google Scholar], [Publisher]
[37]. Jain D., Udhwani T., Sharma S., Gandhe A., Reddy P.B., Nayarisseri A., Singh S.K., *Bioinformation*, 2019, **15**:68 [Crossref], [Google Scholar], [Publisher]
[38]. Zarren G., Shafiq N., Arshad U., Rafiq N., Parveen S., Ahmad Z., *J. Mol. Struct.*, 2021, **1227**:129668 [Crossref], [Google Scholar], [Publisher]
[39]. Adem S., Eyupoglu V., Sarfraz I., Rasul A., Ali M., *preprints*, 2020, 030333 [Crossref], [Google Scholar], [Publisher]
[40]. Akhtar J., Khan A.A., Ali Z., Haider R., Yar M.S., *Eur. J. Med. Chem*., 2017, **125**:143 [Crossref], [Google Scholar], [Publisher]
[41]. Nusrat S., Uzma A., Nazia Y., Jallat K., Ahmad K., Kaynat S., Maryam R., Naila R., Rashid A., Irum J., Sadia N., Muhammad B., *Process Biochem.*, 2021, **104**:152 [Crossref], [Google Scholar], [Publisher]
[42]. Adem S., Eyupoglu V., Sarfraz I., Rasul A., Zahoor A.F., Ali M., Abdalla M., Ibrahim I. M., Elfiky, *Phytomedicine*, 2021, **85**:153310 [Crossref], [Google Scholar], [Publisher]

[43]. Arshad U., Sibtain A., Nusrat S., Zaheer A., Aqsa H., Naseem A., Shagufta P., and Tahir M., *Molecules*, 2021, **26**:4424 [Crossref], [Google scholar], [Publisher]
[44]. Thomsen R., Christensen M.H., Christensen, *J. Med. Chem*., 2006, **49**:3315 [Crossref], [Google Scholar], [Publisher]
[45]. Shah V.R., Bhaliya J.D., Patel G.M., *J. Basic Clin. Physiol. Pharmacol.*, 2021, **32**:197 [Crossref], [Google Scholar], [Publisher]
[46]. Salam P.S., Bolin K.K., *SpringerPlus*, 2012, **1**:1 [Crossref], [Google Scholar], [Publisher]
[47]. Patil R., Das S., Stanley A., Yadav L., Sudhakar A., Varma A.K., *PLoS One*, 2010, **5**:12029 [Crossref], [Google Scholar], [Publisher]
[48]. Maria J.A., Hugo J.C.F., Ana F.T.C., Anabela F.S., Liliana G.O., Sara R.M.O., Rui M.V.A., Manuela P., Isabel C.F.R.F., *Molecules*, 2014, **19**:1672 [Crossref], [Google Scholar], [Publisher]

HOW TO CITE THIS ARTICLE
Mahmood M. Fahad, Nusrat Shafiq, Uzma Arshad, Ali Jabbar Radh. As Antimicrobial Agents: Synthesis, Structural Characterization and Molecular Docking studies of Barbituric Acid Derivatives from Phenobarbital, *Chem. Methodol.*, 2022, 6(2) 122-136
DOI: 10.22034/chemm.2022.2.5
URL: http://www.chemmethod.com/article_141172.html